Science of the Total Environment xxx (xxxx) xxx

Contents lists available at ScienceDirect

Science of the Total Environment

journal homepage: www.elsevier.com/locate/scitotenv

Environmental-friendly coal gangue-biochar composites reclaiming phosphate from water as a slow-release fertilizer

Bing Wang [a,b,c,*], Yuena Ma [d,e], Xinqing Lee [d], Pan Wu [a,b,c], Fang Liu [a,b,c], Xueyang Zhang [f], Ling Li [d], Miao Chen [a,b,c]

[a] College of Resource and Environmental Engineering, Guizhou University, Guiyang 550025, Guizhou, China
[b] Key Laboratory of Karst Environment and Geohazard, Ministry of Natural Resources, Guiyang 550025, Guizhou, China
[c] Guizhou Karst Environmental Ecosystems Observation and Research Station, Ministry of Education, Guiyang, Guizhou 550025, China
[d] State Key Laboratory of Environmental Geochemistry, Institute of Geochemistry, Chinese Academy of Sciences, Guiyang 550081, China
[e] University of Chinese Academy of Sciences, Beijing 100049, China
[f] School of Environmental Engineering, Jiangsu Key Laboratory of Industrial Pollution Control and Resource Reuse, Xuzhou University of Technology, Xuzhou 221018, China

HIGHLIGHTS

- Facile one-step synthesis of coal gangue-modified biochar for the removal of phosphate.
- Coal gangue modified oilseed rape straw biochar show the best adsorption performance.
- Higher pyrolysis temperature and acidic conditions are favorable for phosphate adsorption.
- Adsorption mechanism includes electrostatic adsorption, ligand exchange, and surface precipitation.
- The P-laden biochar composites can promote seed germination and growth.

GRAPHICAL ABSTRACT

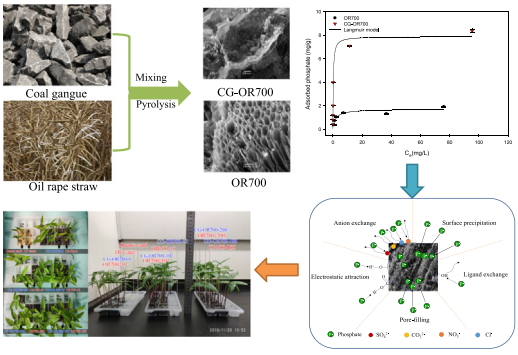

ARTICLE INFO

Article history:
Received 2 August 2020
Received in revised form 22 October 2020
Accepted 1 November 2020
Available online xxxx

Editor: Deyi Hou

Keywords:
Biochar
Phosphate
Coal gangue
Slow-release fertilizer
Wastewater

ABSTRACT

To solve the problem of limited adsorption efficiency of pristine biochar for phosphate, a novel biochar composite was prepared from different feedstocks and coal gangue by one facile-step pyrolysis method. The effects of pyrolysis temperature, adsorbent dosage, pH of the solution, and coexisting ions on phosphate adsorption were analyzed. The adsorption performance and mechanism of phosphate in water were investigated. The application of the phosphorus-laden (P-laden) composite as slow-release fertilizer was evaluated by a germination test. The results showed that the maximum phosphate adsorption capacity of coal gangue modified oilseed rape straw biochar prepared at 700 °C (CG-OR700) was 7.9 mg/g at pH 4.0, which is 4.6 times that of pristine biochar. The adsorption process can be well fitted by the pseudo-second-order kinetic and Langmuir isotherm adsorption model. The mechanism of phosphate adsorption mainly includes surface precipitation, ligand exchange, and electrostatic attraction. The P-laden biochar can be used as a slow-release fertilizer to promote seed germination and growth. This study shows that the coal gangue modified biochar composite can not only be used to remove phosphate from wastewater, but also be used as a slow-release fertilizer, providing a new way for the phosphorus recovery and resource utilization of solid wastes.

* Corresponding author at: College of Resource and Environmental Engineering, Guizhou University, Guiyang 550025, Guizhou, China.
E-mail address: bwang6@gzu.edu.cn (B. Wang).

https://doi.org/10.1016/j.scitotenv.2020.143664
0048-9697/

1. Introduction

The excessive exploitation of phosphate ore resources and the use of a large amount of phosphate fertilizer have caused a series of environmental risks and human health problems (Huang et al., 2017a; Jiao et al., 2012). Phosphorus is one of the main factors leading to eutrophication of waters. Excessive phosphorus is discharged into the water with urban sewage and industrial wastewater, which not only affects the environmental quality of water but also causes huge economic losses (Chen et al., 2020; Conley et al., 2009; Liu et al., 2012). Therefore, how to remove phosphate from water is a hot issue.

At present, the main methods for removing phosphorus from water bodies include biological dephosphorization, chemical precipitation, reverse osmosis, and adsorption methods. Among them, the adsorption method has attracted widespread attention due to its advantages such as high efficiency, simplicity, low economic cost, and good treatment effect. Common adsorption materials for phosphorus include activated carbon, zeolite, molecular sieve, and resin. These adsorbents have the disadvantages of being difficult to separate. As a porous carbonaceous material with a large specific surface area (SSA), biochar is widely used in environmental restoration and soil amendment (Wang et al., 2015; Wang et al., 2018; Xiang et al., 2020; Yu et al., 2019). However, the newly prepared biochar has limited adsorption capacity for anions because of its electronegativity. Consequently, modification of biochar has become an inevitable trend (Rajapaksha et al., 2016; Wang et al., 2017). Different modification methods can obtain different properties of biochar for adsorption and removal of different pollutants. Previous studies have shown that mineral or solid wastes containing calcium, magnesium, iron, etc. have a good effect on biochar modification (Lian et al., 2019; Wang et al., 2019). Among them, Ca, Fe, Mg, Si, Mn, K, and other elements can not only improve its stability, carbon fixation ability and adsorption effect on pollutants (Li et al., 2014; Maroušek et al., 2020), but also the nutrients and metal ions it contains may have a certain positive effect on crops effect. Currently, most studies use various nano-particles, clay minerals, nano-metal oxides, metal salts, and other modified biochar composite materials to adsorb and remove phosphate from water (Ajmal et al., 2020; Cui et al., 2020; Feng et al., 2017). There have been already review papers systematically reviewed the phosphorus uptake and recovery from water with different adsorbents (Bacelo et al., 2020; Huang et al., 2017b; Vikrant et al., 2018). Although these composites have a good adsorption effect, controlling the cost is an important issue to be considered. Therefore, it is necessary to seek low-cost modified composites.

Recently, the modification of biochar using metal-containing solid wastes or natural minerals as a modifying material is receiving increasing attention (Li et al., 2019; Li and Wang, 2019; Lian et al., 2019; Mosa et al., 2020; Qiu and Duan, 2019). Coal gangue, as a solid waste generated during coal mining and washing, not only encroaches on a large number of land resources but also poses certain risks to the environment. It is reported that the cumulative amount of coal gangue piled up in China has reached 6 billion tons, and the annual discharge amount is about 500–800 million tons. Therefore, how to make effective use of it is an urgent problem to be solved. At present, the utilization of coal gangue is mainly concentrated in fields such as construction materials, agriculture, and energy. The main ingredients in coal gangue include SiO_2, Al_2O_3, Fe_2O_3, MgO, and CaO. The previous research results show that phosphorus absorption by using MgO and CaO-modified biochar composites or can be used as a slow-release fertilizer (Liu et al., 2019; Wu et al., 2019; Yao et al., 2013; Zhang et al., 2012; Zheng et al., 2019). As a kind of metal-rich solid waste, coal gangue may change the functional groups, surface charges of biochar after co-pyrolysis with other biomass, thus affecting its adsorption capacity for pollutants. To utilize coal gangue effectively and comprehensively, a novel biochar composite was prepared from different feedstocks and coal gangue by one facile-step pyrolysis method. We assume that the biochar modified by coal gangue could be used for the removal of anions such as phosphate in water.

To explore the adsorption effect and mechanism of coal gangue modified biochar on phosphate in water, batch adsorption experiments were carried out. Seed germination and seedling growth tests were performed to evaluate the potential of P- laden biochar as a slow-release fertilizer. The objectives of this research were to: (1) prepare coal gangue modified biochar composites and characterize their physicochemical properties; (2) study on the adsorption behavior and mechanism of phosphate by gangue modified biochar; (3) evaluate the effect of P-laden biochar composites on seed germination and growth.

2. Materials and methods

2.1. Materials

All the chemicals and reagents are analytical grade, which include: potassium dihydrogen phosphate (KH_2PO_4), sulfuric acid (H_2SO_4), ascorbic acid, anhydrous sodium carbonate, 2, 4-dinitrophenol, antimony potassium tartrate, ammonium molybdate, nitric acid, hydrochloric acid. The background solution is deionized (DI) water.

2.2. Preparation of CG-biochar composite

The coal gangue used in this study was sampled from a typical coal gangue stacking site in Liupanshui City, Guizhou Province, China. The oilseed rape, maize, and rice straws were sampled from the suburban of Guiyang City. Distillers' grains were collected from a local liquor enterprise. For the preparation of pristine biochar, the methods and conditions are similar to our previous studies (Wang et al., 2019). Biochar was prepared using a tube furnace under 450 °C and 700 °C, respectively. For the preparation of CG-biochar, the coal gangue is crushed into less than 2 cm by a crusher, and then ball-milled for 3 h with water. After ball milling, it is dried at 80 °C, and the agglomerated coal gangue powder is fully ground into powder. Then, the raw materials and coal gangue were mixed in a wet 2:1 mass method, soaked with water and stirred evenly and dried at 80 °C to obtain modified biochar raw materials. The modified biochar is produced in the same way as the pristine biochar mentioned above. The different pristine biochars prepared at different temperatures were labeled as oilseed rape (OR450 and OR 700), maize straw (MS450 and MS700), distillers' grains (DG450 and DG700) and rice straws (RS450 and RS700), while the different coal gangue modified biochar prepared at different temperatures were labeled as oilseed rape (CG-OR450 and CG-OR 700), maize straw (CG-MS450 and CG-MS700), distillers' grains (CG-DG450 and CG-DG700) and rice straw (CG-RS450 and CG-RS700). The number after the capital letter represents the pyrolysis temperature.

2.3. Characterization of adsorbents

The pH of biochar, SEM, FTIR, BET, Zeta potential, and elemental composition were analyzed according to our previous study (Lian et al., 2019). The determination of moisture, volatiles, and ash refers to the method of (ASTM, 2007). SSA was measured by an SSA analyzer (Kubo X1000, Beijing bio Electronic Technology Co., Beijing, China). pH value was measured by pH meter (pHS—3C, Shanghai Leici instrument Co., LTD.). The conductance was measured with a conductivity meter (HI 8733, HANNA). SEM-EDS characterization using scanning electron microscopy (JSM-IT300, Japan electronics Co., Ltd.) to observe the surface morphology and analyze the elemental components. FTIR was used to determine the functional groups (Thermofisher, Nicolet iS10, USA). Thermogravimetric analysis (TGA) was performed to determine the thermal stability of biochar at a heating rate of 10 °C/min in N_2 ambient. Organic element analysis was performed using an organic element analyzer (Vario EL cube, Germany). The zeta potential of biochar was measured at room temperature by using Malvern Zetasizer Nano ZSE (Malvern Instruments, UK).

2.4. Adsorption experiments

To screen out the best feedstocks and pyrolysis temperature, 0.5 g biochar samples were put into a 50 mL centrifuge tube, then 40 mL 50 mg/L KH_2PO_4 solution was added and then put onto a shaker for 200 r/min. After shaking for 24 h, the samples were immediately filtered with a 20–25 μm filter. Then the concentration of phosphate in the solution was determined by UV spectrophotometry. Based on the optimal pyrolysis temperature and feedstock from the above experiments, to figure out the effect of different dosage on phosphate adsorption, 0.05, 0.1, 0.2, 0.5 and 1 g of biochar from rape and maize were weighed at 700 °C respectively, using the same experimental procedures as described above.

The effects of different solution pH values on phosphate adsorption were carried out. The pH value of 100 mg/L KH_2PO_4 solution was adjusted from 3 to 11, respectively. Kinetic adsorption experiments were performed by sampling at different time intervals of 0.083, 0.25, 0.5, 1, 2, 4, 8, 16, and 24 h for phosphate analysis. The adsorption isotherm experiment was conducted by analyzing different phosphate concentrations of 5, 10, 15, 25, 50, 100, and 200 mg/L KH_2PO_4 solution at pH 4.0 shaking for 24 h. Adsorption kinetics and isotherm experiments were performed under pH 4.0 and the dosage of 0.5 g. The TGA spectrum of different biochar composites, the effects of dosage, different adsorption models, and fitting parameters of adsorption kinetics and isotherms are provided in Supporting information (SI).

2.5. Seed germination and seedling growth

2.5.1. Experimental seed treatment

Market-bought mung bean seeds (*Phaseolus aureus*) were washed with DI water, disinfected with 70% ethanol, and soaked for 10 min. After washing with DI water, the seeds were immersed in DI water for 3 h.

2.5.2. Substrate treatment

The P-laden biochar from the adsorption isotherm experiment was put into the oven to dry at 60 °C. AR grade 40–80 mesh quartz sand was washed five times with DI water and put into the oven for drying at 80 °C. The above P-laden biochar and pristine biochar were mixed in a 3.5 × 3.5 × 2.8 cm plastic box at a ratio of 1:10 between biochar and quartz sand, and 10 g quartz sand and DI water were taken as blank control.

2.5.3. Incubation

Three treated mung bean seeds were placed in each box. The seeds were completely covered in the medium. Place the plastic box in a greenhouse and water it three times a day to keep the medium moist. The condition of germination and growth was recorded by taking photos and measuring growth every day, and the plants were taken out for statistical analysis after 14 days.

3. Results and discussion

3.1. Characterization of the samples

The physicochemical properties of pristine and CG-biochars were shown in Table 1. It can be seen that all biochar are alkaline, in which the highest pH of CG-OR700 is 11.93 and the lowest pH of OR450 is 9.04. This is because plants can accumulate certain bases in the growth process, and these bases could be concentrated during the pyrolysis process, thus the pH value of biochar increases with the increase of pyrolysis temperature (Tomczyk et al., 2020). Besides, due to the presence of K, Na, Ca, Mg, Al, Fe and other alkaline ions in the gangue, the biochar and modified biochar obtained from pyrolysis are alkaline (Hassan et al., 2020). The SSA of CG-RS700 is the largest, which is 157.32 m^2/g, followed by CG-OR700, which is 144.59 m^2/g. The SSA of CG-OR700 is 118.5 times that of OR700, which has a positive impact on phosphate adsorption. In general, the SSA and pore volume of modified biochar is much higher than that of pristine biochar, which indicates that the surface and pore structure of biochar is significantly improved by the modified treatment. The zeta potential of all biochar is generally negative, which shows that the four biochar surfaces are negatively charged, and the negative charge of biochar at 700 °C is slightly higher than that at 450 °C, and the negative charge of biochar modified by coal gangue is significantly reduced, which is conducive to the adsorption of phosphate.

The SEM images of pristine biochar and CG-biochar composites prepared from different feedstocks and temperatures were shown in Fig. 1. It can be seen that biochars prepared from four kinds of feedstocks at 700 °C show a different morphology and pore structures. After coal gangue modification, the flocculent particles of coal gangue are attached to the surface of biochar or embedded in the pores of biochar, which makes the adsorption active site fully exposed and further increases the adsorption of phosphate. It indicates that the chemical reactions between coal gangue and different biomass during the pyrolysis process directly affect the physicochemical properties, element composition, specific surface area, and porosity of biochar.

FTIR spectra of different biochars were shown in Fig. 2. The peak with wavenumber 1065 cm^{-1} may be a C—O functional group. The bending vibration of Si-O-Fe produced a characteristic peak of

Table 1
Physiochemical properties of pristine biochar and CG- biochars.

Adsorbent	Biochar	pH	Zeta potential (mV)	EC (μs cm^{-1})	BET-SAA (m^2/g)	Pore volume (cm^3 g^{-1})	BJH pore size (nm)	Elemental contents						Ash %	Volatile %
								C wt%	H wt%	N wt%	S wt%	H/C_{tot} mol mol^{-1}	C/N ratio		
Pristine biochar	OR450	9.55	−20.78	1344	4.17	0.003069	1.47	72.59	3.26	1.35	0.51	0.54	62.73	6.29	71.20
	OR700	10.58	−30.08	11,670	1.22	0.000921	1.51	75.53	1.99	1.17	0.44	0.32	75.31	11.07	67.69
	DG450	10.1	−13.09	1387	12.28	0.001556	0.25	66.75	3.03	5.18	0.25	0.54	15.03	20.22	58.07
	DG700	9.84	−13.64	1265	0.27	0.000417	3.04	69.07	1.7	4.22	0.22	0.30	19.10	21.38	56.50
	RS450	10.65	−18.50	85,200	5.95	0.003943	1.32	49.23	2.97	0.76	0.18	0.72	75.57	33.19	61.32
	RS700	10.70	−11.63	87,100	3.71	0.002341	1.26	47.79	1.86	0.73	0.17	0.47	76.38	34.57	56.84
	MS450	10.20	−13.13	7470	1.07	0.000746	1.39	72.97	3.37	1.64	0.24	0.55	51.91	9.9	50.42
	MS700	11.38	−8.09	19,460	3.24	0.001815	1.12	69.45	1.88	1.09	0.42	0.32	74.33	16.1	49.92
CG-biochar	CG-OR450	9.04	−22.82	1056	7.92	0.004555	1.15	19.98	1.22	0.39	0.82	0.73	59.77	29.51	64.39
	CG-OR700	11.93	−6.00	2520	144.59	0.068881	0.95	17.13	0.6	0.25	0.78	0.42	79.94	55.04	43.91
	CG-DG450	9.81	−10.37	2040	7.18	0.004507	1.25	17.75	1.21	1.25	0.7	0.82	16.57	67.1	32.75
	CG-DG700	10.38	−7.63	2720	48.07	0.023236	0.97	19.35	0.67	0.71	1.33	0.42	31.80	44.44	41.85
	CG-RS450	10.70	−7.35	28,400	37.76	0.016418	1.03	18.89	1.06	0.35	0.68	0.67	62.97	50.32	49.37
	CG-RS700	10.17	−19.82	14,700	157.32	0.076818	0.98	14.36	0.55	0.2	0.93	0.46	83.77	57.63	38.87
	CG-MS450	9.84	−9.55	2440	8.58	0.004621	1.08	23.76	1.43	0.54	0.73	0.72	51.33	40.3	46.15
	CG-MS700	11.40	−13.14	9980	91.44	0.044111	0.96	18.19	0.73	0.28	1.36	0.48	75.79	52.54	41.64

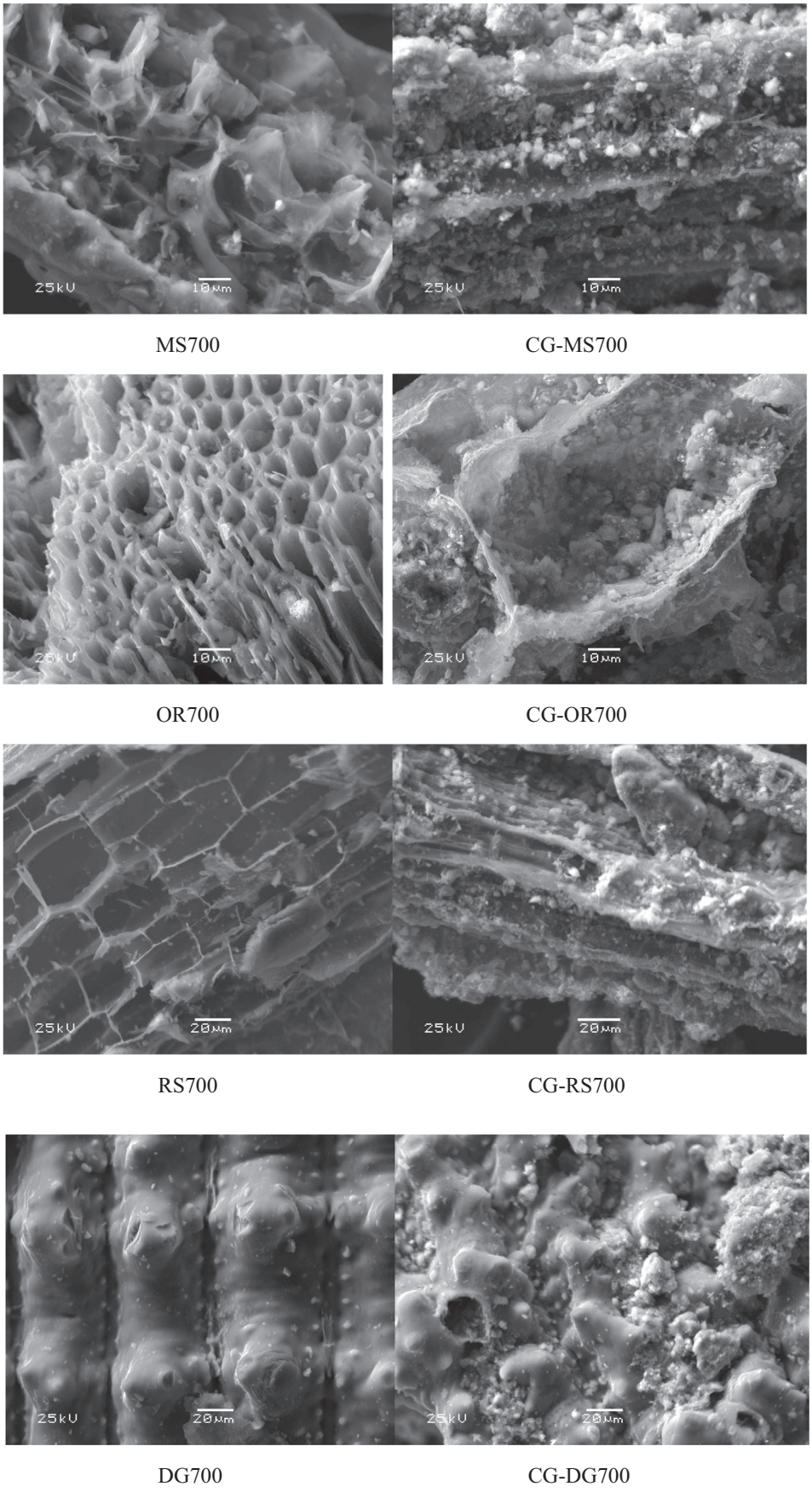

Fig. 1. The SEM images of pristine biochar and CG-biochar composites prepared from different feedstocks pyrolyzed under 700 °C.

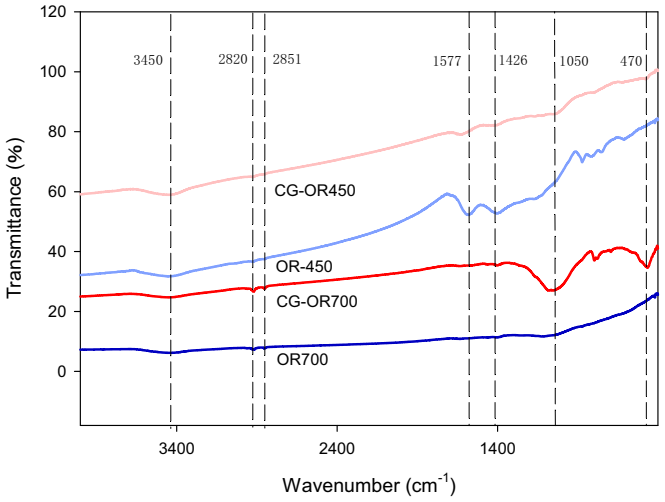

Fig. 2. The FTIR spectra of OR 450, CG-OR450, OR 700 and CG-OR700.

470 cm^{-1}, indicating that Fe was successfully embedded into biochar. The higher peak value indicates higher Fe content. The metal oxides on the surface of the modified biochar are active sites for phosphate adsorption. Therefore, the adsorption performance of the modified biochar is better than that of the pristine biochar.

The thermo-gravimetric analysis (TGA) spectrum of OR450, OR700, CG-OR450, and CG-OR700 are shown in Fig. S1. TGA shows that the pyrolysis process of OR450 and OR 700 is almost the same, mainly including three stages: The first stage curve is relatively smooth, which is the thermal stability stage. The stage from room temperature to 250 °C is mainly the loss of water in biomass, with a weight loss rate of about 2%; the stage from 250 °C to 500 °C is when cellulose, hemicellulose and some lignin are pyrolyzed, generating a large number of volatile substances, a small amount of tar and carbon; the stage higher than 500 °C is mainly the pyrolysis of residual lignin. The process is very slow and carbon is mainly formed after pyrolysis. After 500 °C, the thermogravimetry curve and pyrolysis rate curve tend to be gentle, and the weight loss almost has no obvious change, indicating that the biochar has been carbonized completely. For CG-OR700, the pattern was similar to CG-OR450 except that higher temperature decomposition was delayed indicating that thermal stability was improved after incorporation with CG.

3.2. Influencing factors

3.2.1. Effect of pyrolysis temperature

Pyrolysis temperature directly affects the physicochemical properties of biochar, thus affecting its adsorption capacity for pollutants (Wang et al., 2016). As shown in Fig. S2, with the increase of pyrolysis temperature, the adsorption capacity of biochar to phosphate increases, indicating that high pyrolysis temperature is conducive to the adsorption of phosphate by biochar which is consistent with our previous studies (Wang et al., 2019). This is mainly because the metal ions in coal gangue are more likely to react with the functional groups on the surface of biochar under high pyrolysis temperature, making the pores more developed and the SSA larger. Previous studies have also found that the SSA and pore structure of biochar are changed by pyrolysis with minerals or metal-containing solid waste (Li et al., 2014; Lian et al., 2019).

3.2.2. Effect of adsorbent dosage

As shown in Fig. S3, with the increase of the dosage, the adsorption capacity of coal gangue modified biochar on phosphate gradually decreases, while the removal rate has been increasing. When the dosage is 0.05–0.2 g, the initial adsorption capacity decreases obviously, and when the dosage is 0.2–0.5 g, the changing trend slows down, while the removal rate increases rapidly, reaching about 80%. This is because when the dosage is low, the adsorption potential of the adsorbent is easy to reach saturation, so its adsorption capacity is high. However, due to the limited adsorption potential, there is not enough adsorption point to absorb the phosphate in the water, so the removal rate of phosphate in the water is not high. With the increase of dosage, more phosphate is adsorbed in the water, which leads to the rapid increase of removal rate and the decrease of adsorption (Wang et al., 2019). When the dosage is 0.5 g, the removal rate is about 80%. Therefore, from the perspective of economy and cost, 0.5 g can be considered as the optimal dosage.

3.2.3. Effect of solution pH

It can be seen from Fig. S4a that the adsorption capacity of OR700 and CG-OR700 to phosphate under different pH values. In general, pH had little effect on the adsorption of OR700 to phosphate, and the fluctuation of adsorption capacity was not obvious under different pH conditions. For CG-OR700, the adsorption capacity of phosphate is different under different pH conditions. The adsorption capacity under acid condition is higher than that under alkaline conditions. This is because the main forms of phosphate are $H_2PO_4^-$ and HPO_4^{2-} in an acid condition. It can be seen from Fig. S4b that the fluctuation trend of the zeta potential of OR700 is similar to CG-OR700 under different pH values. Generally, with the increase of pH value, zeta potential gradually decreases. For OR700, the zeta potential remains negative in the range of 3.0–11.0. For CG-OR700, the zeta potential is positive in the range of pH 3.0–7.0, negative in the range of pH 7.0–11.0, and the zero potential is 7.0. Therefore, CG-OR700 is positively charged under acidic conditions, which is more favorable for the adsorption of phosphate. The biochar with positive charges has electrostatic adsorption with phosphate in aqueous solution. With the increase of solution pH, the positive charge on the surface of CG-OR700 decreased, which was not conducive to phosphate adsorption. When the point of zero charge (PZC) reaches at pH 7.0, there is no electrostatic adsorption between biochar surface and phosphate. When pH > 7.0, the main forms of phosphate are $H_2PO_4^-$ and PO_4^{3-}. However, the electrostatic repulsion of negatively charged CG-OR700 with $H_2PO_4^-$, PO_4^{3-} in aqueous solution makes it difficult for $H_2PO_4^-$ and PO_4^{3-} to adsorb on the surface of CG-OR700 (Vikrant et al., 2018).

3.2.4. Effect of coexisting ions

Various anions often exist in the water environment, which could interfere with the adsorption behavior of phosphate on adsorbents. To further study and evaluate the adsorption performance of the composite in the actual situation, we simulated the competitive adsorption

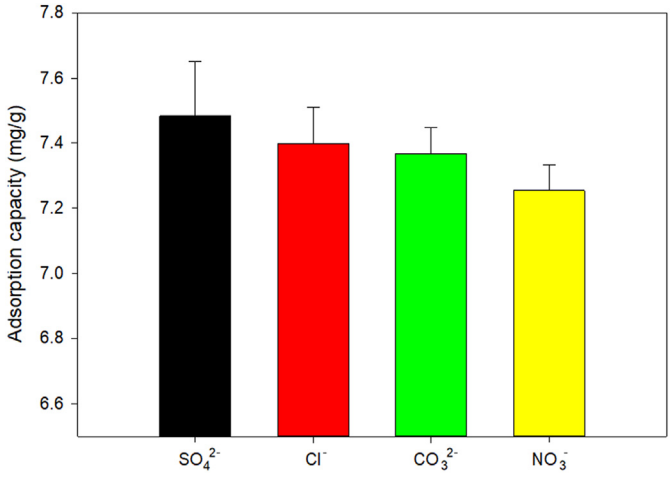

Fig. 3. The effect of coexisting ions on phosphate adsorption.

Table 2
The maximum adsorption capacities of phosphate onto various biochars.

Biochar	Temperature (°C)	Q_0 (mg/g)	pH	References
Mixed hardwood feedstock biochar	300	1.13	–	(Sarkhot et al., 2013)
Wheat straw	450	16.58	7.0	(Li et al., 2016)
Peanut shell biochar	700	6.79	7.0	(Jung et al., 2015)
Iron rich sludge biochar	300	1.843	–	(Wang et al., 2020)
Magnetic water hyacinth biochar	450	5.07	–	(Cai et al., 2017)
Feimpregnated wood chip-derived biochar	500	3.201	–	(Michalekova-Richveisova et al., 2017)
Magnetite/orange peel biochar	700	1.242	–	(Chen et al., 2011)
Fly ash-biochar	500	3.08	–	(Qiu and Duan, 2019)
Coal gangue-biochar	500	3.20	–	(Qiu and Duan, 2019)
CG-OR700	700	7.9	–	This study

between several common anions in sewage. As shown in Fig. 3, the order of influence intensity of different anions is $NO_3^- > CO_3^{2-} > Cl^- > SO_4^{2-}$. With the increase of ion type and ion intensity, the phosphate adsorption capacity of coal gangue modified biochar in water slightly decreases, but the effect of reduction is not obvious. The results show that the effect of coexisting ions on phosphorus adsorption is limited, which is consistent with previous research results (Jia et al., 2020). This is mainly due to the strong binding ability of phosphate to the surface of CG-OR700. There is no obvious competitive adsorption when other anions coexist, which indicates that the CG-OR700 biochar can be applied to the removal of phosphorus in actual water.

3.3. Adsorption kinetics

As shown in Fig. S5, in the first 4 h, the adsorption rate was very fast. This is because there are a lot of phosphate adsorption sites on the surface of biochar composite at the initial stage. With the increase of adsorption time, the adsorption rate slows down obviously between 4 and 8 h, indicating that most of the adsorption potential has been occupied. From 8 to 16 h, the adsorption capacity changed smoothly and reached the adsorption equilibrium in 24 h.

Different kinetic models were used to fit the kinetic curves. It can be seen from Table S1 that the fitting correlation coefficient R^2 of the pseudo-second-order kinetic model for CG-OR700 is the highest, which indicates that the pseudo-second-order kinetic model can better describe the phosphate adsorption process. The equilibrium adsorption amount calculated by the pseudo-second-order kinetic model is consistent with the actual equilibrium adsorption amount. The results showed that the adsorption of phosphate on coal gangue modified biochar was mainly chemical adsorption. This is also verified by other modified biochars in previous studies (Yin et al., 2018).

3.4. Adsorption isotherms

Fig. S6 shows the phosphate adsorption isotherms of CG-OR700. The adsorption capacity increased with the increase of initial concentration. Under the condition of the low initial concentration of phosphate, the phosphate adsorption capacity increased rapidly. With the increase of initial concentration of phosphate, the adsorption capacity gradually reached equilibrium. This is because the surface-active sites of coal gangue modification are gradually occupied with the increase of phosphate concentration, thus reaching saturation state. The fitting parameters of different adsorption models are shown in Table S2. It can be seen that the correlation coefficient of Langmuir fitting is higher than that of the Freundlich model, indicating that the Langmuir adsorption model can more accurately fit the adsorption process of phosphate on CG-OR700, so the adsorption belongs to single molecular layer adsorption. The maximum adsorption capacity is 7.9 mg/g, which is 4 times higher than that before modification. The k_L value after modification was significantly higher than that before modification, which indicated that the ability of phosphate-binding was promoted.

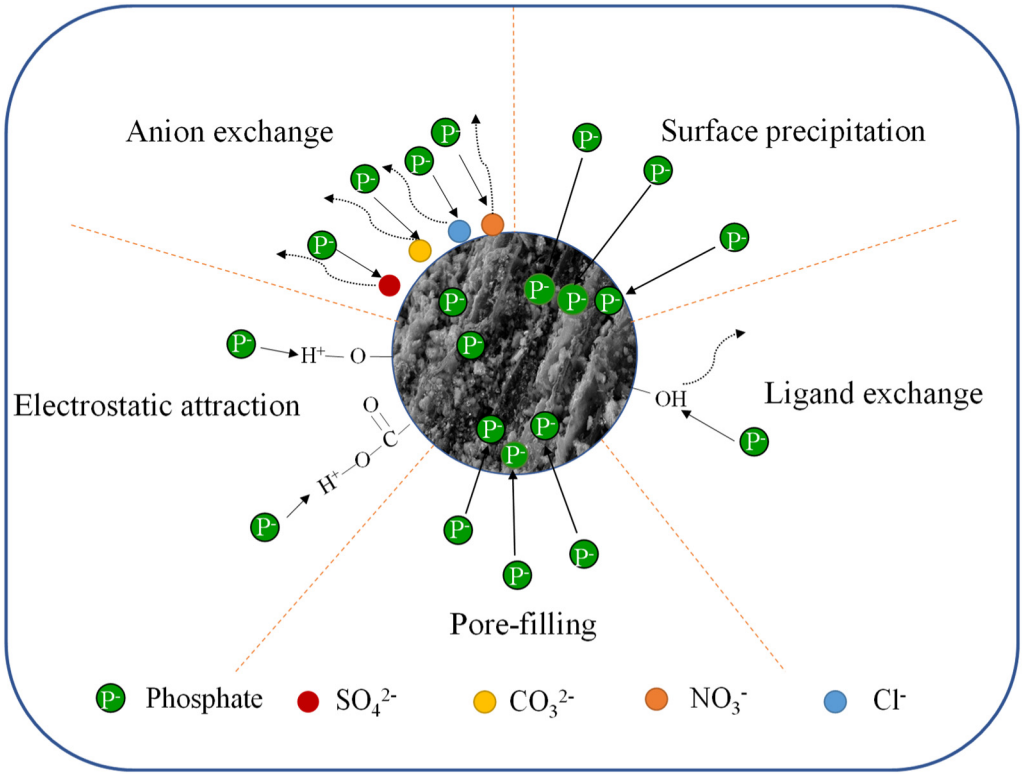

Fig. 4. The mechanisms of phosphate adsorption onto coal gangue modified biochar.

Although the phosphate adsorption capacity of CG biochar is not as high as that of other modified biochar (Table 2), it is prepared from two kinds of solid wastes. Therefore, from the perspective of environmental friendliness, CG biochar can effectively utilize solid wastes, and it has low production cost and simple operation. Therefore, the adsorbent has a certain application prospect and value.

3.5. Adsorption mechanisms

Previous studies have found that there are several mechanisms for phosphate adsorption by carbonaceous materials, mainly including ion exchange, ligand exchange, surface complexation and precipitation, and electrostatic attraction (Vikrant et al., 2018). In this study, the phosphate adsorption of coal gangue modified biochar can be attributed to three main mechanisms: electrostatic adsorption, ligand exchange, and surface precipitation (Fig. 4).

The SEM-EDS of OR700 and CG-OR700 were shown in Fig. 5. After coal gangue modification, the content of Si and Fe increased significantly, Si increased by 2–3% under the same treatment, and Fe content in the original biochar was almost zero, but it was 2–5% after modification. This shows that the biochar successfully loaded Si and Fe through coal gangue modification, which is consistent with the result of the FTIR in Fig. 2. The main reason for adsorption is the formation of Fe (Ca)-O-P bond on the surface of coal gangue modified biochar.

As biochar is negatively charged, it has limited or no adsorption capacity for phosphate. Previous studies have shown that ligand exchange is one of the main mechanisms of phosphate adsorption. The zeta potential of coal gangue modified biochar showed that at pH 3.0–7.0, the surface of CG-OR700 was positively charged, so there was an electrostatic attraction between CG-OR700 and negatively charged phosphate. Therefore, the mechanism of phosphate removal in acid conditions included ligand exchange and electrostatic adsorption. When pH 7.0, it is the zero potential point of coal gangue modified biochar. At this time, there is no electrostatic effect between coal gangue modified biochar and phosphate. Therefore, the mechanism of phosphate adsorption is mainly ligand exchange at pH 7.0, while at pH > 7.0, when the surface of coal gangue modified biochar is negatively charged, there is electrostatic repulsion between the coal gangue modified biochar and the negatively charged phosphate, so in the alkaline condition, the ligand exchange is the main mechanism of phosphate adsorption by CG-OR700.

4. Seed germination and growth

It can be seen from Fig. 6 that the P-laden biochar composites can promote the germination and growth of seeds to a certain extent. In general, the effect of CG-OR700 with more phosphate adsorbed on crop growth was significantly higher than that with less phosphate. The results indicated that the absorbed phosphate was bioavailable (Wang et al., 2020). It is likely released and absorbed by plants during the germination process, which played the role of slow-release fertilizer. It can also be seen from Fig. 6 that the more phosphate the modified biochar is absorbed, the more obvious it is in promoting the

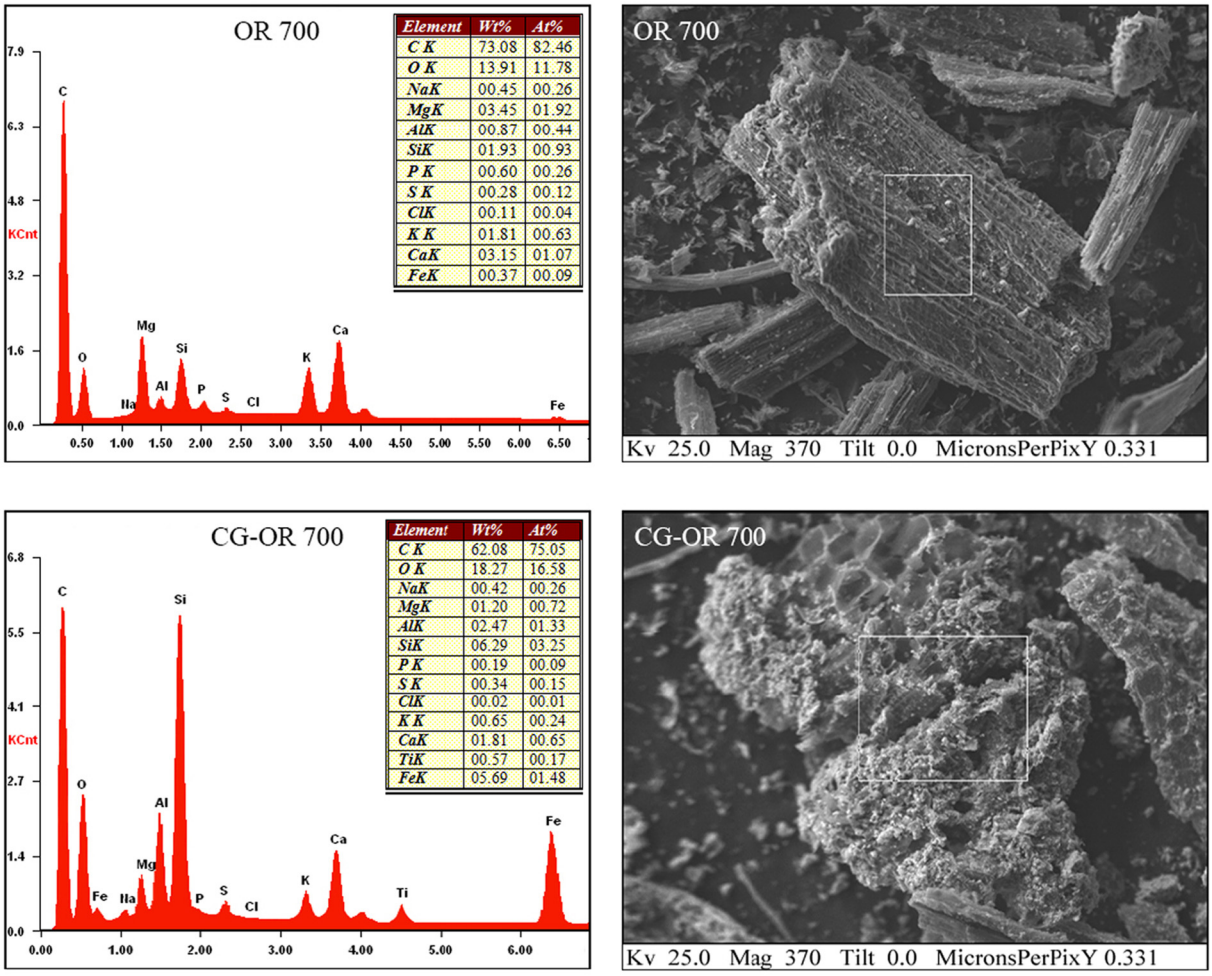

Fig. 5. The SEM-EDS of OR700 and CG-OR700.

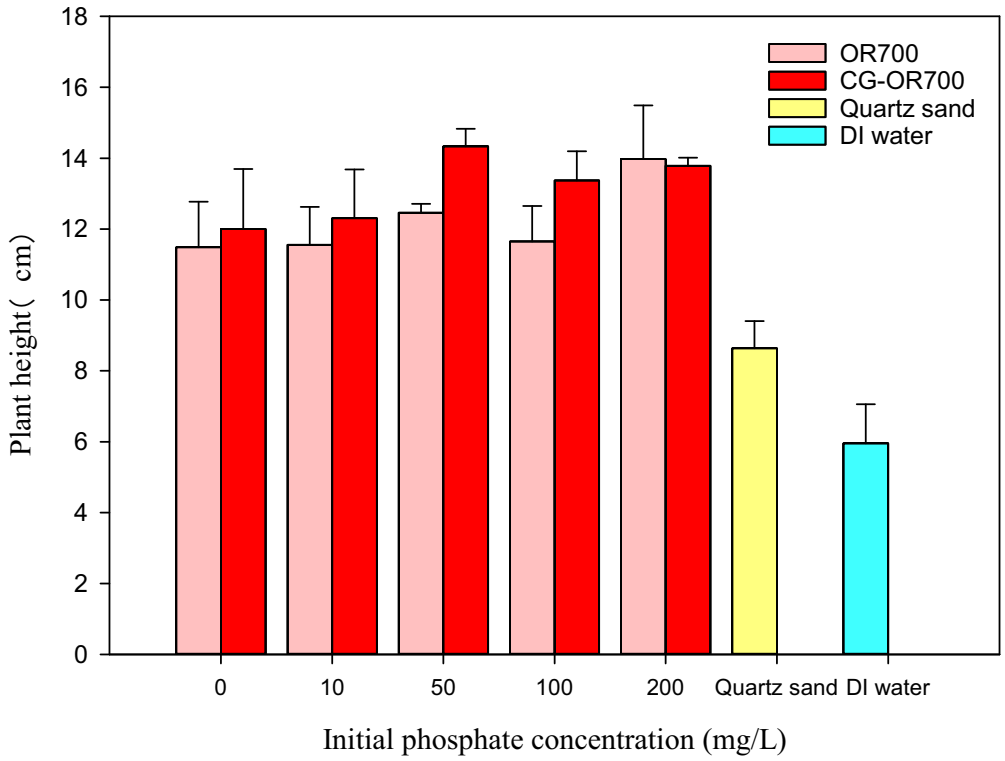

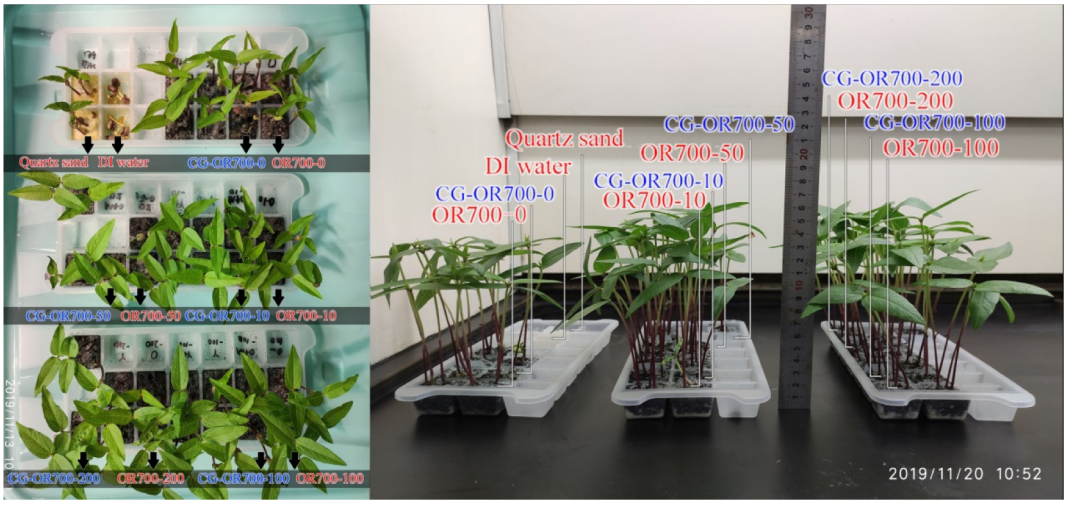

Fig. 6. The effect of biochar composite with different phosphorus loading on seed germination and growth under different initial concentrations (mg/L).

growth of plants, and there are significant differences between different treatments. Different types of agricultural soils will be used to carry out planting experiments of different crops to evaluate their long-term effectiveness in the future.

5. Conclusions

Coal gangue modification can promote the adsorption of phosphate on biochar, and high pyrolysis temperature can improve the adsorption capacity of coal gangue modified biochar. The best adsorption performance can be achieved by adding 2.5 g/L dosage under acid conditions. The adsorption process is following the second-order kinetics and Langmuir model. The maximum adsorption capacity is about 4 times higher than that of the pristine biochar. The adsorption mechanism mainly includes electrostatic adsorption, ligand exchange, and surface precipitation. The P-laden biochar composite can be used as a slow-release fertilizer, which can promote the germination and growth of plants. This study shows that the biochar modified by coal gangue not only realizes the resource utilization of solid waste, but also reduces the production cost of the biochar composite. It can be applied to the removal of phosphate in water and agricultural production, and truly realizes the recycling of solid waste.

Credit author statement

Bing Wang: Supervision, Conceptualization, Methodology, Writing-Reviewing and Editing. **Yuena Ma**: Experiment, Analysis, Methodology. **Xinqing Lee**: Supervision, Writing- Reviewing and Editing. **Pan Wu**: Writing- Reviewing and Editing. **Fang Liu**: Writing- Reviewing and Editing. **Xueyang Zhang**: Analysis. **Ling Li**: Reviewing and Editing. **Miao Chen**: Reviewing and Editing.

Declaration of competing interest

The authors declare that they have no known competing financial interests or personal relationships that could have appeared to influence the work reported in this paper.

Acknowledgments

This work was supported by the National Key Research and Development Program of China (2016YFC0502602), the National Natural Science Foundation of China (41977297), the High-Level Overseas Talent Innovation and Entrepreneurship Project of Guizhou Province [(2018)08] and the Special Research Fund of Natural Science (Special Post) of Guizhou University [(2020)01].

Appendix A. Supplementary data

Supplementary data to this article can be found online at https://doi.org/10.1016/j.scitotenv.2020.143664.

References

Ajmal, Z., Muhmood, A., Dong, R., Wu, S., 2020. Probing the efficiency of magnetically modified biomass-derived biochar for effective phosphate removal. J. Environ. Manag. 253, 109730.

ASTM, 2007. D1762-84 Standard Test Method for Chemical Analysis of Wood Charcoal. ASTM International, West Conshohocken,PA.

Bacelo, H., Pintor, A.M.A., Santos, S.C.R., Boaventura, R.A.R., Botelho, C.M.S., 2020. Performance and prospects of different adsorbents for phosphorus uptake and recovery from water. Chem. Eng. J. 381, 122566.

Cai, R., Wang, X., Ji, X.H., Peng, B., Tan, C.Y., Huang, X., 2017. Phosphate reclaim from simulated and real eutrophic water by magnetic biochar derived from water hyacinth. J. Environ. Manag. 187, 212–219.

Chen, B., Chen, Z., Lv, S., 2011. A novel magnetic biochar efficiently sorbs organic pollutants and phosphate. Bioresour. Technol. 102, 716–723.

Chen, X.-X., Liu, Y.-M., Zhao, Q.-Y., Cao, W.-Q., Chen, X.-P., Zou, C.-Q., 2020. Health risk assessment associated with heavy metal accumulation in wheat after long-term phosphorus fertilizer application. Environ. Pollut. 262, 114348.

Conley, D.J., Paerl, H.W., Howarth, R.W., Boesch, D.F., Seitzinger, S.P., Havens, K.E., et al., 2009. Controlling eutrophication: nitrogen and phosphorus. Science 323.

Cui, Q., Xu, J., Wang, W., Tan, L., Cui, Y., Wang, T., et al., 2020. Phosphorus recovery by core-shell γ-Al_2O_3/Fe_3O_4 biochar composite from aqueous phosphate solutions. Sci. Total Environ. 729, 138892.

Feng, Y., Lu, H., Liu, Y., Xue, L., Dionysiou, D.D., Yang, L., et al., 2017. Nano-cerium oxide functionalized biochar for phosphate retention: preparation, optimization and rice paddy application. Chemosphere 185, 816–825.

Hassan, M., Liu, Y., Naidu, R., Parikh, S.J., Du, J., Qi, F., et al., 2020. Influences of feedstock sources and pyrolysis temperature on the properties of biochar and functionality as adsorbents: a meta-analysis. Sci. Total Environ. 744, 140714.

Huang, W., Zhang, Y., Li, D., 2017a. Adsorptive removal of phosphate from water using mesoporous materials: a review. J. Environ. Manag. 193, 470–482.

Huang, J., Xu, C.-c., Ridoutt, B.G., Wang, X.-C., Ren, P.-a., 2017b. Nitrogen and phosphorus losses and eutrophication potential associated with fertilizer application to cropland in China. J. Clean. Prod. 159, 171–179.

Jia, Z., Zeng, W., Xu, H., Li, S., Peng, Y., 2020. Adsorption removal and reuse of phosphate from wastewater using a novel adsorbent of lanthanum-modified platanus biochar. Process Saf. Environ. Prot. 140, 221–232.

Jiao, W., Chen, W., Chang, A.C., Page, A.L., 2012. Environmental risks of trace elements associated with long-term phosphate fertilizers applications: a review. Environ. Pollut. 168, 44–53.

Jung, K.W., Hwang, M.J., Ahn, K.H., Ok, Y.S., 2015. Kinetic study on phosphate removal from aqueous solution by biochar derived from peanut shell as renewable adsorptive media. Int. J. Environ. Sci. Technol. 12, 3363–3372.

Li, J., Wang, J., 2019. Comprehensive utilization and environmental risks of coal gangue: a review. J. Clean. Prod. 239, 117946.

Li, F., Cao, X., Zhao, L., Wang, J., Ding, Z., 2014. Effects of mineral additives on biochar formation: carbon retention, stability, and properties. Environmental Science & Technology 48, 11211–11217.

Li, J., Lv, G., Bai, W., Liu, Q., Zhang, Y., Song, J., 2016. Modification and use of biochar from wheat straw (Triticum aestivum L.) for nitrate and phosphate removal from water. Desalin. Water Treat. 57, 4681–4693.

Li, J., Li, B., Huang, H., Lv, X., Zhao, N., Guo, G., et al., 2019. Removal of phosphate from aqueous solution by dolomite-modified biochar derived from urban dewatered sewage sludge. Sci. Total Environ. 687, 460–469.

Lian, G., Wang, B., Lee, X., Li, L., Liu, T., Lyu, W., 2019. Enhanced removal of hexavalent chromium by engineered biochar composite fabricated from phosphogypsum and distillers grains. Sci. Total Environ. 697, 134119.

Liu, C., Kroeze, C., Hoekstra, A.Y., Gerbens-Leenes, W., 2012. Past and future trends in grey water footprints of anthropogenic nitrogen and phosphorus inputs to major world rivers. Ecol. Indic. 18, 42–49.

Liu, X., Shen, F., Qi, X., 2019. Adsorption recovery of phosphate from aqueous solution by CaO-biochar composites prepared from eggshell and rice straw. Sci. Total Environ. 666, 694–702.

Maroušek, J., Kolář, L., Strunecký, O., Kopecký, M., Bartoš, P., Maroušková, A., et al., 2020. Modified biochars present an economic challenge to phosphate management in wastewater treatment plants. J. Clean. Prod. 272, 123015.

Michalekova-Richveisova, B., Fristak, V., Pipiska, M., Duriska, L., Moreno-Jimenez, E., Soja, G., 2017. Iron-impregnated biochars as effective phosphate sorption materials. Environ. Sci. Pollut. Res. 24, 463–475.

Mosa, A., El-Ghamry, A., Tolba, M., 2020. Biochar-supported natural zeolite composite for recovery and reuse of aqueous phosphate and humate: batch sorption–desorption and bioassay investigations. Environmental Technology & Innovation 19, 100807.

Qiu, B., Duan, F., 2019. Synthesis of industrial solid wastes/biochar composites and their use for adsorption of phosphate: from surface properties to sorption mechanism. Colloids Surf. A Physicochem. Eng. Asp. 571, 86–93.

Rajapaksha, A.U., Chen, S.S., Tsang, D.C., Zhang, M., Vithanage, M., Mandal, S., et al., 2016. Engineered/designer biochar for contaminant removal/immobilization from soil and water: potential and implication of biochar modification. Chemosphere 148, 276–291.

Sarkhot, D., Ghezzehei, T., Berhe, A., 2013. Effectiveness of biochar for sorption of ammonium and phosphate from dairy effluent. J. Environ. Qual. 42, 1545–1554.

Tomczyk, A., Sokołowska, Z., Boguta, P., 2020. Biochar physicochemical properties: pyrolysis temperature and feedstock kind effects. Rev. Environ. Sci. Biotechnol. 19, 191–215.

Vikrant, K., Kim, K.-H., Ok, Y.S., Tsang, D.C.W., Tsang, Y.F., Giri, B.S., et al., 2018. Engineered/designer biochar for the removal of phosphate in water and wastewater. Sci. Total Environ. 616-617, 1242–1260.

Wang, B., Lehmann, J., Hanley, K., Hestrin, R., Enders, A., 2015. Adsorption and desorption of ammonium by maple wood biochar as a function of oxidation and pH. Chemosphere 138, 120–126.

Wang, B., Lehmann, J., Hanley, K., Hestrin, R., Enders, A., 2016. Ammonium retention by oxidized biochars produced at different pyrolysis temperatures and residence times. RSC Adv. 6, 41907–41913.

Wang, B., Gao, B., Fang, J., 2017. Recent advances in engineered biochar productions and applications. Crit. Rev. Environ. Sci. Technol. 47, 2158–2207.

Wang, Q., Wang, B., Lee, X., Lehmann, J., Gao, B., 2018. Sorption and desorption of Pb(II) to biochar as affected by oxidation and pH. Sci. Total Environ. 634, 188–194.

Wang, B., Lian, G., Lee, X., Gao, B., Li, L., Liu, T., et al., 2019. Phosphogypsum as a novel modifier for distillers grains biochar removal of phosphate from water. Chemosphere 238, 124684.

Wang, H., Xiao, K., Yang, J., Yu, Z., Yu, W., Xu, Q., et al., 2020. Phosphorus recovery from the liquid phase of anaerobic digestate using biochar derived from iron−rich sludge: a potential phosphorus fertilizer. Water Res. 174, 115629.

Wu, L., Wei, C., Zhang, S., Wang, Y., Kuzyakov, Y., Ding, X., 2019. MgO-modified biochar increases phosphate retention and rice yields in saline-alkaline soil. J. Clean. Prod. 235, 901–909.

Xiang, W., Zhang, X., Chen, J., Zou, W., He, F., Hu, X., et al., 2020. Biochar technology in wastewater treatment: a critical review. Chemosphere 252, 126539.

Yao, Y., Gao, B., Chen, J., Yang, L., 2013. Engineered biochar reclaiming phosphate from aqueous solutions: mechanisms and potential application as a slow-release fertilizer. Environmental Science & Technology 47, 8700–8708.

Yin, Q., Ren, H., Wang, R., Zhao, Z., 2018. Evaluation of nitrate and phosphate adsorption on Al-modified biochar: influence of Al content. Sci. Total Environ. 631-632, 895–903.

Yu, H., Zou, W., Chen, J., Chen, H., Yu, Z., Huang, J., et al., 2019. Biochar amendment improves crop production in problem soils: a review. J. Environ. Manag. 232, 8–21.

Zhang, M., Gao, B., Yao, Y., Xue, Y., Inyang, M., 2012. Synthesis of porous MgO-biochar nanocomposites for removal of phosphate and nitrate from aqueous solutions. Chem. Eng. J. 210, 26–32.

Zheng, Y., Wang, B., Wester, A.E., Chen, J., He, F., Chen, H., et al., 2019. Reclaiming phosphorus from secondary treated municipal wastewater with engineered biochar. Chem. Eng. J. 362, 460–468.